Microsomal prostaglandin E synthase 1 determines tumor growth in vivo of prostate and lung cancer cells

Hiromi Hanaka[a], Sven-Christian Pawelzik[b,1], John Inge Johnsen[c,1], Marija Rakonjac[a], Kan Terawaki[a], Agnes Rasmuson[c], Baldur Sveinbjörnsson[c,d], Martin C. Schumacher[e], Mats Hamberg[a], Bengt Samuelsson[a,2], Per-Johan Jakobsson[b], Per Kogner[c], and Olof Rådmark[a,2]

[a]Department of Medical Biochemistry and Biophysics, Division of Physiological Chemistry II, [b]Rheumatology Unit, Department of Medicine, [c]Childhood Cancer Research Unit, Department of Woman and Child Health, and [e]Department of Urology, Karolinska Institutet, S-171 77 Stockholm, Sweden; and [d]Department of Biology and Histological Institute of Medical Biology, University of Tromsö, N9037 Norway

Contributed by Bengt Samuelsson, September 10, 2009 (sent for review June 17, 2009)

There is strong evidence for a role of prostaglandin E_2 (PGE_2) in cancer cell proliferation and tumor development. In PGE_2 biosynthesis, cyclooxygenases (COX-1/COX-2) convert arachidonic acid to PGH_2, which can be isomerized to PGE_2 by microsomal PGE-synthase-1 (MPGES-1). The human prostate cancer cell line DU145 expressed high amounts of MPGES-1 in a constitutive manner. MPGES-1 expression also was detectable in human prostate cancer tissues, where it appeared more abundant compared with benign hyperplasia. By using shRNA, we established stable and practically complete knockdown of MPGES-1, both in DU145 cells with high constitutive expression and in the non-small cell lung cancer cell line A549, where MPGES-1 is inducible. For microsomes prepared from knockdown clones, conversion of PGH_2 to PGE_2 was reduced by 85–90%. This resulted in clear phenotypic changes: MPGES-1 knockdown conferred decreased clonogenic capacity and slower growth of xenograft tumors (with disintegrated tissue structure) in nude mice. For DU145 cells, MPGES-1 knockdown gave increased apoptosis in response to genotoxic stress (adriamycin), which could be rescued by exogenous PGE_2. The results suggest that MPGES-1 is an alternative therapeutic target in cancer cells expressing this enzyme.

arachidonic acid | cyclooxygenase | eicosanoid | prostaglandin E2

Prostaglandin E_2 (PGE_2) is an eicosanoid with many functions; its role as a mediator of pain and fever in inflammatory reactions is of major importance. In PGE_2 biosynthesis, cyclooxygenases (COX-1, COX-2) transform arachidonic acid to the endoperoxide PGG_2, which is reduced to PGH_2. Subsequently, PGE synthase (PGES) converts PGH_2 into PGE_2. Three PGESs are present in human cells: two microsomal and one cytosolic (also referred to as p23, a cofactor for Hsp90). Microsomal PGE_2 synthase-1 (MPGES-1), belonging to the MAPEG family, is inducible by proinflammatory stimuli, such as IL-1β and LPS. As for COX-2, this induction is reduced by anti-inflammatory glucocorticoids (1–4). See Samuelsson et al. (5) for a recent review on MPGES-1.

For many cancer cells, production of COX and lipoxygenase-derived eicosanoids promotes growth and survival (6, 7). Increased amounts of PGE_2 were first found in colorectal adenomas and cancers, and nonsteroidal anti-inflammatory drugs (NSAIDs) that inhibit COX reduce the risk of developing colorectal cancer. However, COX-2 inhibitors are associated with cardiovascular side effects (for review, see refs. 5 and 8). Not only COX-2 but also high expression of MPGES-1 has been found in various cancers, including non-small cell lung cancer, colorectal cancer, breast cancer, and hepatocellular carcinoma (5). However, for prostate cancer cell lines as well as tissue, different observations have been made regarding expression of COX-2 (up- or down-regulation in relation to normal prostate epithelial cells and tissue; see refs. 9 and 10 for reviews). Interestingly, during proliferative inflammatory atrophy, which may precede prostate cancer, COX-2 was up-regulated (11), and NSAIDs may prevent development of benign prostatic hyperplasia (12). Recently, inhibition of cytosolic phospholipase A_2 (provides arachidonic acid for eicosanoid biosynthesis) in the prostate cancer cell line PC3 was found to reduce xenograft tumor growth (13).

PGE_2 promotes cancer cell growth and survival by several mechanisms, including increased proliferation, counteracted apoptosis, increased migration and invasiveness, angiogenesis, recruitment of myeloid suppressor cells to evade T-cell attack, and chronic inflammation. These effects are mediated via multiple signaling pathways, including cross-talk with Wnt and EGFR pathways (6, 8–10, 14–16). Thus, PGE_2 has been implied in many different types of cancer, and COX inhibitors are tested in animal models for cancer (e.g., neuroblastoma; ref. 17) and in the clinic regarding prostate cancer (10). Here, we show that the human prostate cancer cell line DU145 expresses large amounts of MPGES-1. Knockdown of MPGES-1 by shRNA gave considerably reduced tumorigenicity of both DU145 and the human lung cancer cell line A549. MPGES-1 was also detected in prostate cancer tissue samples.

Results

High Constitutive Expression of MPGES-1 in DU145 Cells. Three human prostate cancer cell lines (DU145, PC3, and LNCaP) were analyzed for MPGES-1 protein expression (Fig. 1*A*). High expression was found in DU145 cells. Comparison to known amounts of purified MPGES-1 protein on Western blots gave an estimate of about 10 ng per 100 μg of total protein. Weaker expression of MPGES-1 was found in PC3 cells, and in LNCaP samples MPGES-1 protein was not detectable. For the human lung adenocarcinoma cell line A549, up-regulation of MPGES-1 by IL-1β was confirmed (Fig. 2*A*). However, IL-1β did not change expression of MPGES-1 in the prostate cancer cell lines (Fig. S1). Hence, the high expression in DU145 is constitutive. Samples from DU145 cells typically showed more intense bands at 16,000 than analogous samples from A549 cells that had been treated with IL-1β, as illustrated in Fig. 2*A*.

A similar pattern was obtained when MPGES-1 enzyme activity was determined by incubations of microsomes with PGH_2 (10 μM

Author contributions: H.H., J.I.J., M.R., B. Samuelsson, P.K., and O.R. designed research; H.H., S.-C.P., J.I.J., M.R., K.T., A.R., B. Sveinbjörnsson, M.C.S., and M.H. performed research; M.H. and P.-J.J. contributed new reagents/analytic tools; H.H., S.-C.P., J.I.J., M.R., K.T., A.R., B. Sveinbjörnsson, M.C.S., P.-J.J., P.K., and O.R. analyzed data; and H.H., S.-C.P., J.I.J., P.K., and O.R. wrote the paper.

The authors declare no conflict of interest.

Freely available online through the PNAS open access option.

[1]S-C.P. and J.I.J. contributed equally to this work.

[2]To whom correspondence may be addressed. E-mail: bengt.samuelsson@ki.se or olof.radmark@ki.se.

This article contains supporting information online at www.pnas.org/cgi/content/full/0910218106/DCSupplemental.

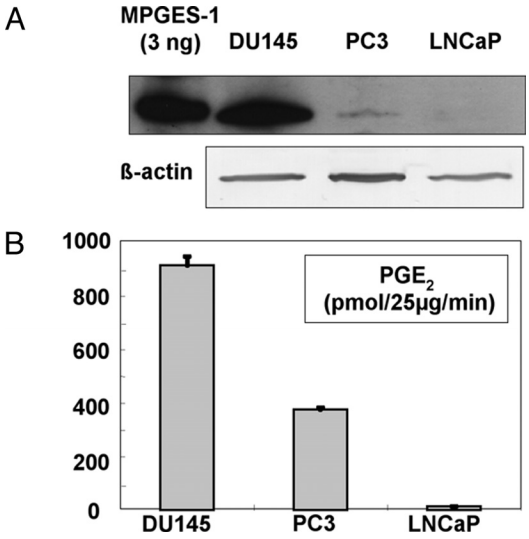

Fig. 1. Analyses of MPGES-1 in three prostate cancer cell lines. (*A*) For Western blot cells growing on dishes were lysed with M-PER buffer, and 37.5-μg aliquots of total cellular protein were applied to SDS/PAGE gels. For loading controls (β-actin), 7.5-μg aliquots were analyzed. After electroblotting, membranes were incubated with antibodies to MPGES-1 and β-actin (see *Materials and Methods*). (*B*) Conversion of PGH_2 to PGE_2 by microsomal proteins prepared from three prostate cancer cell lines. Cells were detached by addition of trypsin/EDTA for 10 min at 37 °C and were collected by centrifugation. After sonication, membrane-bound proteins (microsomes) were prepared (see *Materials and Methods*). Aliquots (25 μg) in 100 μL were incubated with PGH_2 (10 μM) for 1 min on ice. After solid-phase extraction, samples were analyzed by HPLC-UV (195 nm). Activity is given as picomoles of PGE_2 formed per 25 μg of protein per minute ± SE (n = 3).

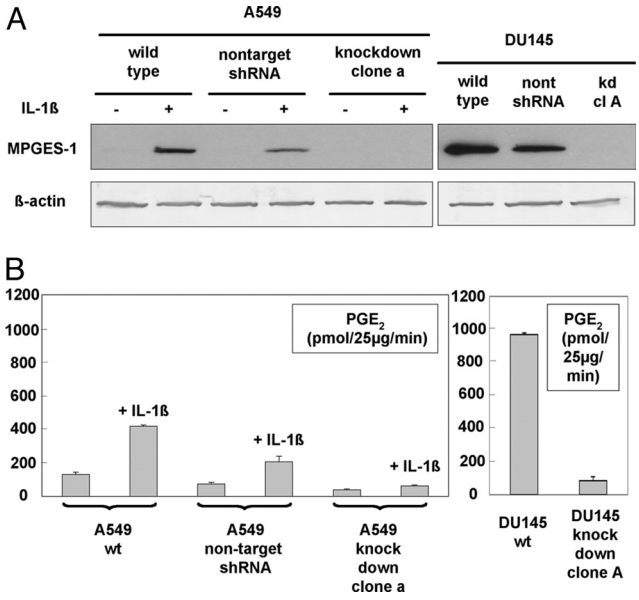

Fig. 2. Analyses of MPGES-1 in DU145 and A549 knockdown clones. (*A*) Western blots. For DU145, samples were prepared for WT, cells transfected with negative control nontargeting shRNA plasmid, and DU145 knockdown clone A. For A549, WT, negative control, and knockdown clone a were cultured with or without IL-1β (1 ng/mL) for 72 h. Cells were lysed with M-PER buffer, and 37.5-μg aliquots of total protein were applied to SDS/PAGE gels. β-Actin analyses show equal loading. After electroblotting, membranes were incubated with antibodies to MPGES-1 and β-actin (see *Materials and Methods*). For both MPGES membranes, autoradiography exposure time was 1 min. (*B*) Conversion of PGH_2 to PGE_2 by microsomal proteins prepared from WT and knockdown clones. For DU145, samples were prepared for WT and knockdown clone A. For A549, WT, cells transfected with negative control nontargeting shRNA plasmid, and A549 knockdown clone a were cultured with or without IL-1β (1 ng/mL) for 72 h. Cells were detached by addition of trypsin/EDTA for 10 min at 37 °C and were collected by centrifugation. After sonication, membrane-bound proteins (microsomes) were prepared as described in *Materials and Methods*. Aliquots (25 μg) in 100 μL were incubated with PGH_2 (10 μM) for 1 min on ice. After solid-phase extraction, samples were analyzed by HPLC-UV (195 nm). Activity is given as picomoles of PGE_2 formed per 25 μg of protein per min ± SE (n = 3–5).

for 1 min on ice). The highest activity (914 pmol PGE_2 formed per 25 μg of microsomal protein per minute) was found for DU145, followed by PC3 and LNCaP (Fig. 1*B*). Please note that in the incubations of DU145 microsomes, almost all substrate was converted, limiting PGE_2 formation. Thus, the MPGES-1 activity of DU145 microsomes is probably underestimated. This may also explain the apparently high MPGES-1 activity in PC3 microsomes in relation to the Western blot bands.

Generation of Stable MPGES-1 Knockdown Cells. In view of the high expression of MPGES-1 in DU145, this prostate cancer cell line was used for RNAi. For comparison, we also performed RNAi for MPGES-1 in A549 cells. Cells were transfected with five different shRNA plasmids by using Lipofectamine 2000, and stable transfectants were selected by resistance to puromycin. For DU145, clone A was found to be a practically complete knockdown clone, and this clone was used in the experiments described below. For A549, the selected complete knockdown clone was denoted clone a. The absence of MPGES-1 protein in the knockdown clones is shown in Fig. 2*A*. For A549 knockdown clone a, MPGES-1 was absent also after stimulation with IL-1β. After transfections with the negative control nontargeting shRNA plasmid, MPGES-1 was still expressed. These knockdown clones (DU145 knockdown clone A, A549 knockdown clone a) are stable; no MPGES-1 protein expression has been detectable up to 1.5 years after initial isolation. For DU145, efficient knockdown was demonstrated also by quantitative PCR. For WT DU145, the MPGES-1 to cyclophilin A (PPIA) mRNA ratio was 7%. For DU145 knockdown clone A, this was reduced to 0.3%. Expression of PPIA, considered a stable reference gene, was the same in WT and knockdown cells.

Knockdown was demonstrated also by MPGES-1 activity assays (Fig. 2*B*). For DU145 knockdown clone A, formation of PGE_2 from PGH_2 was reduced by 90% compared with WT DU145. For A549 knockdown clone a, formation of PGE_2 from PGH_2 was reduced by 85% compared with WT A549 (cells treated with IL-1β). As shown, MPGES-1 activity remained inducible by IL-1β in A549 transfected with the negative control shRNA plasmid. In a separate experiment, MPGES-1 activity was demonstrated also for DU145 transfected with this negative control. The constitutive MPGES-1 activity was higher for WT DU145 compared with WT A549 treated with IL-1β (Fig. 2*B*).

Expression of COX-2 in A549 and DU145 Cells. As previously published (2–4), expression of COX-2 protein in A549 cells was strongly induced by IL-1β, whereas for noninduced cells, COX-2 expression was weak (or not detectable). As observed previously (18), COX-2 expression in DU145 cells was relatively weak, but with some variation, as shown in Fig. 3. Treatment with IL-1β (1 ng/mL; 24 h) resulted in a slightly increased COX-2 Western blot band for DU145 cells, but not to the same extent as for A549 (Fig. 3). After 24 h, TNF-α (10 ng/mL) had no effect on COX-2 expression in DU145, although COX-2 in A549 increased about 2- to 3-fold. COX-2 was found also in the MPGES-1 knockdown clones (both A549 and DU145); no correlation could be observed regarding expression of these two enzymes (Fig. S2).

Subcellular Localization of MPGES-1 and COX-2 in A549 and DU145 Cells. By using confocal microscopy and double stain, subcellular localization of MPGES-1 and COX-2 was determined before and after cell stimulation with IL-1β. For A549, the intensity of both

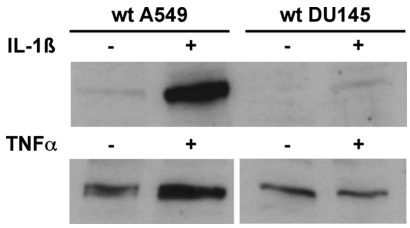

Fig. 3. Western blot analyses of COX-2 in WT DU145 and A549 cells. (*Upper*) cells were cultured with or without IL-1β (1 ng/mL) for 24 h. (*Lower*) cells were cultured with or without TNF-α (10 ng/mL) for 24 h. Cells were lysed with M-PER buffer, and 37.5-μg aliquots of cellular protein were applied to SDS/PAGE gels. After electroblotting, membranes were incubated with COX-2 antibody (see *Materials and Methods*).

MPGES-1 and COX-2 was higher for stimulated cells, in accordance with Western blotting. Staining was most intense around the nucleus, fading off toward the cell periphery. Colocalization (yellow) of MPGES-1 and COX-2 can be observed, particularly around nuclei in cells stimulated with IL-1β (Fig. S3*A*). Thus, the general view that these two enzymes function together in biosynthesis of PGE_2 is supported by the immunocytochemistry pattern in A549 cells.

For DU-145 cells, strong staining for MPGES-1 was seen in nonstimulated cells and in cells stimulated with IL-1β (Fig. S3*B*). However, the localization appears more distinctly perinuclear in IL-1β-stimulated cells. A weak but similarly perinuclear ring can also be observed for COX-2 after IL-1β. The two enzymes thus colocalize also in DU145 cells, although the much stronger signal for MPGES-1 (green) compared with COX-2 (red) yields a less clear composite yellow, compared with A549 cells (Fig. S3*A*).

Inhibition of MPGES-1 Expression Impairs DU145 and A549 Clonogenicity. Clonogenic assay was performed to determine whether MPGES-1 expression determines the tumorigenic potential of DU145 and A549 cells. In both cell lines, the clonogenic capacity was significantly reduced ($P < 0.001$) in cells stably transfected with shRNA against MPGES-1 (Fig. 4*A*). The reduction was more pronounced for A549 knockdown cells (23% of WT) compared with DU145 knockdown cells (47% of WT). After transfection with the negative control nontargeting shRNA plasmid, there was a slight reduction of DU145 clonogenicity, but not so for A549 cells. These results indicate a less malignant phenotype after MPGES-1 knockdown.

Knockdown of MPGES-1 Reduces the Tumorigenic Potential of DU145 and A549 Cells in Vivo. Next, we investigated the effect of MPGES-1 knockdown on tumor development in vivo. DU145 and A549 WT tumor cells, nontargeting shRNA control cells, and MPGES-1 knockdown cells were injected into hind flanks of nude mice, and tumor formation was monitored. The time to tumor take, defined as the number of days for a tumor in the animal to reach a volume of 0.2 mL, was prolonged after knockdown of MPGES-1 for both DU145 and A549 knockdown cells. For DU145 knockdown clone A, the median time to tumor volume 0.2 mL was more than doubled compared with WT cells (53 vs. 18 days; Fig. 5*B*). In addition, DU145 knockdown clone A cells did not develop tumors in 48% of the injection sites (Fig. 4*B*). For A549 cells, similar results were obtained. Only 5 of 20 injections of A549 knockdown clone resulted in tumors (0.2 mL) at the end of the experiment, 72 days after tumor cell injection (Fig. 4*C*). When mice were injected with cells (DU145, A549) transfected with negative control nontargeting shRNA plasmid, tumor growth was not significantly delayed. These results show that MPGES-1 is important for the tumorigenic potential of these cells.

The histology of DU145 xenografts was examined. Tumors

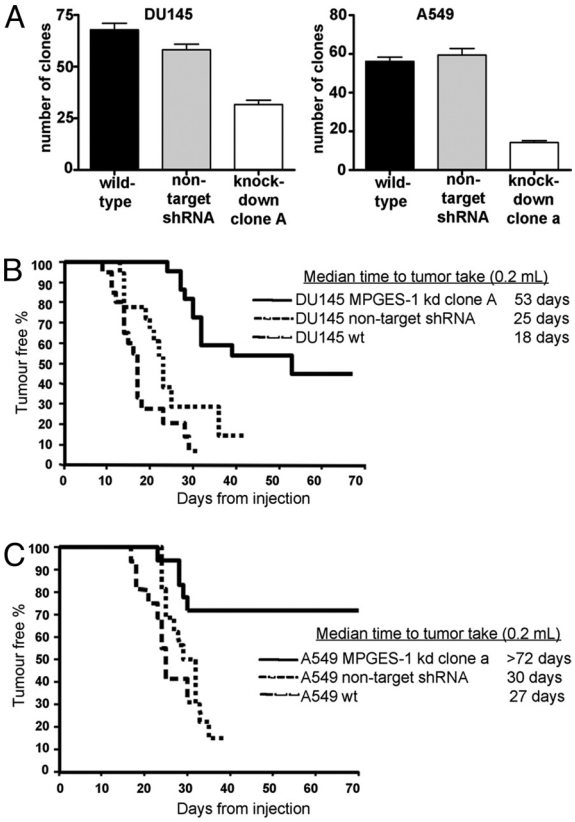

Fig. 4. Tumorigenic potential of wild type cells and MPGES-1 knockdown clones. (*A*) Clonogenic survival of DU145 and A549 MPGES-1 knockdown clones. Cells were seeded in six-well Cell+ plates and incubated for 12 days in complete growth medium. Colonies (>75 cells) with 50% plate efficiency were counted. Six parallel plates for each cell type and variant were performed, and number of clones ± SE is shown. (*B* and *C*) Knockdown of MPGES-1 impairs the tumorigenic potential of DU145 and A549 cells. Kaplan–Meier curves showing the percentage of tumor-free injection sites from the day of tumor cell injection. (*B*) NMRI nu/nu mice (10 in each group) were injected in both hind flanks with DU145 cells. A significant delay in tumor development was observed in mice xenografted with the MPGES-1 knockdown clone A compared with DU145 WT cells ($P < 0.005$) or compared with cells transfected with nontargeting shRNA ($P < 0.005$). (*C*) NMRI nu/nu mice (10 in each group) were injected in both hind flanks with A549 cells. A significant delay in tumor development was observed in mice xenografted with the MPGES-1 knockdown clone a compared with A549 WT cells ($P < 0.005$) or compared with cells transfected with nontargeting shRNA ($P < 0.005$).

growing from DU145 WT cells consisted of homogeneous viable tumor tissue, whereas MPGES-1 knockdown DU145 cells tumors displayed large areas with massive necrosis and nonviable tumor parenchyma (hematoxylin/eosin stain; Fig. S4*A*). DU145 WT tumors contained Ki-67-positive cells throughout, whereas there was only a small rim of viable cells (Ki-67^+) along the periphery of the MPGES-1 knockdown tumor (Fig. S4*B*).

Expression of MPGES-1 and COX-2 in Xenograft Tumors. Expression of MPGES-1 and COX-2 in excised xenograft tumor tissues was analyzed by Western blot analyses. Reduced expression of MPGES-1 was detected in tumors derived from DU145 knockdown clone A, compared with tumors derived from WT cells and from DU145 transfected with nontarget shRNA (Fig. 5*A*). For A549 cells, expression of MPGES-1 was similar in all xenograft tumors (Fig. 5*B*). These observations suggest that the xenograft tumor tissues (DU145, A549) contain different amounts of stromal and endothelial cells that express MPGES-1. Also, COX-2 was present in all tumors and most abundant in xenografts from A549 cells (in which COX-2 is highly inducible).

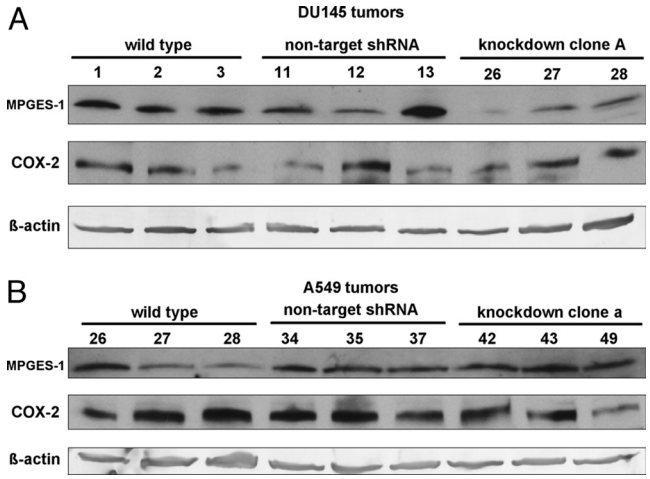

Fig. 5. Western blot analyses of MPGES-1 in xenograft tumor tissues. Tumors were excised from the injection sites (hind flanks) of NMRI nu/nu mice and snap-frozen in liquid nitrogen. Pieces of frozen tissue were solubilized (M-PER plus sonication), and aliquots (37.5 μg) of total protein were applied to SDS/PAGE gels. After electroblotting, membranes were incubated with antibodies to MPGES-1, COX-2, and β-actin (see *Materials and Methods*). (*A*) Tumors derived from DU145 cells. (*B*) Tumors derived from A549 cells.

Expression of MPGES-1, COX-2, and Androgen Receptor in Prostate Tissue Samples. Cancer and benign hyperplasia tissues were obtained from prostate surgery. From pieces of frozen tissue, Western blot samples were prepared (Fig. 6, five cancer with Gleason grade 6 or 7, and five benign; see Table 1). Expression of MPGES-1 was clearly detectable in two of the prostate cancer samples (nos. 6 and 9), whereas weaker bands were observed for the remaining three cancer samples. In four of the five benign hyperplasia samples, MPGES-1 was undetectable; only in sample 4 could a very faint band be observed. Thus, from these 10 samples, MPGES-1 appears to be more abundant in prostate cancer tissue compared with benign hyperplasia. Expression of COX-2 was seen in four of the benign samples and in three of the cancer samples. Thus, COX-2 varied in prostate tissue samples, as published previously (9, 10). Androgen receptor was clearly detected in four of the benign samples and in four of the cancer samples.

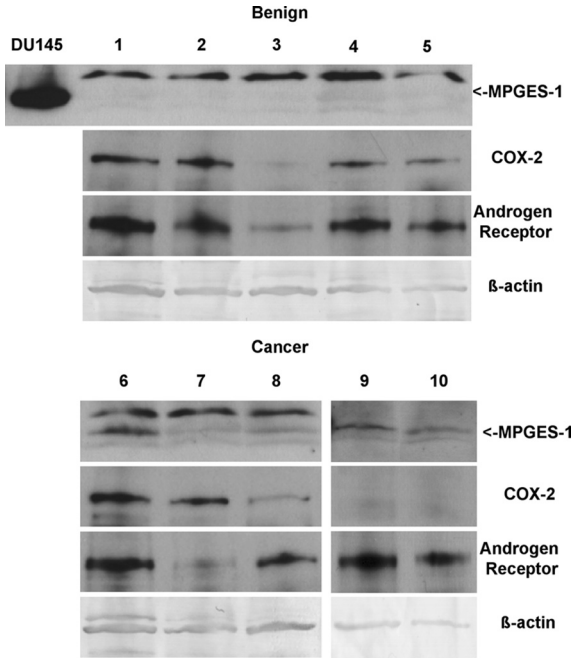

Fig. 6. Western blot analyses of prostate tissues (five cancer and five benign hyperplasia). Samples were prepared from frozen tissues as described in *Materials and Methods*. For analysis of MPGES-1 in lanes 1–8, 200 μg of protein was applied to SDS/PAGE gels, and Cayman antibody no. 160140 was used. For lanes 9–10, 80 μg of protein was applied, and the in-house MPGES-1 antibody was used. For analysis of COX-2 and androgen receptor, 37.5 μg was analyzed. For antibodies, see *Materials and Methods*.

Table 1. Donors of prostate tissues analyzed in Fig. 6

Sample, no.*	Age, y	Preoperative PSA in plasma, ng/mL	Gleason score of the prostatectomy specimen
1 b	59.2	7.2	–
2 b	56.6	6.8	–
3 b	50.2	3.9	–
4 b	61.9	2.7	–
5 b	73.5	18	–
6 c	44.7	19	4+3=7
7 c	70.5	5.4	3+4=7
8 c	58.6	17	3+4=7
9 c	70.9	4.3	3+3=6
10 c	56.7	0.8	3+3=6

PSA indicates for prostate-specific antigen.
*In this column, b indicates benign, and c indicates cancer.

MPGES-1 Knockdown Sensitizes DU145 Cells to Adriamycin. Caspase activation after treatment with adriamycin reflects apoptosis by the intrinsic (mitochondria-dependent) pathway (19). As indicated by the 6-fold increase in accumulated cytokeratin 18 fragments, genotoxic stress-induced apoptosis was considerably increased after knockdown of MPGES-1 in DU145 cells (Fig. 7*A*). Interestingly,

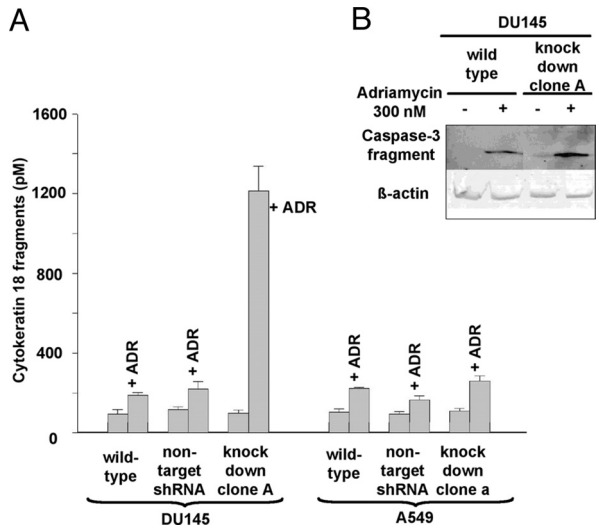

Fig. 7. Adriamycin-induced apoptosis in wild type cells and MPGES-1 knockdown clones. (*A*) Apoptosis assay. Cells (7×10^3) were seeded on 96-well plates and allowed to attach for 24 h. New medium containing 300 nM adriamycin was added, and after 24 h cells were lysed, and cytokeratin 18 fragments were analyzed by ELISA. For each condition, two incubations were analyzed ($n = 2$), and results are given $\pm$ SD. (*B*) Western blot analysis of caspase-3 fragment in DU145 cells—WT and MPGES-1 knockdown clone A—after treatment with adriamycin (300 nM) for 24 h. Cells were lysed with M-PER buffer, and 50-μg aliquots of total protein were applied to the SDS/PAGE gel. β-Actin analysis shows equal loading. After electroblotting, the membrane was incubated with an antibody for caspase-3 cleaved at Asp-175.

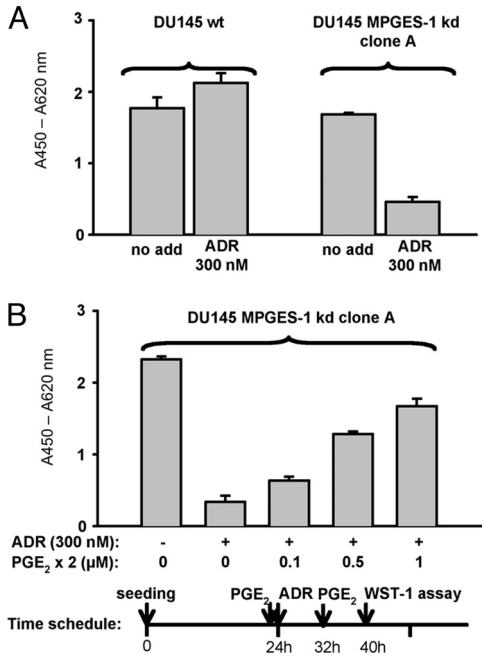

Fig. 8. Proliferation of wild type DU145 cells and MPGES-1 knockdown clone A, effect of adriamycin. (*A*) Cells were seeded on 96-well plates (10×10^3 cells per well). At 24 h after seeding, adriamycin (300 nM) was added. After an additional 24 h, cell viability was determined by mitochondrial dehydrogenase assay (cleavage of the tetrazolium salt WST-1; $n = 2$). (*B*) PGE_2 augments proliferation of DU145 MPGES-1 knockdown cells in the presence of adriamycin. Cells were seeded on 96-well plates (5×10^3 cells per well), and 24 h after seeding, adriamycin (300 nM) was added. PGE_2 was added twice, as indicated. After a total 40 h, cell viability was determined by WST-1 assay ($n = 2$).

this was not the case for A549 cells. In DU145 MPGES-1 knockdown cells, there was also an increased amount of activated caspase-3 fragment after treatment with adriamycin (Fig. 7*B*). Similar results were obtained regarding DU145 cell viability. DU145 MPGES-1 knockdown cells were sensitive to adriamycin, whereas WT cells were resistant (Fig. 8*A*). Addition of exogenous PGE_2 could rescue DU145 MPGES-1 knockdown cells against the effect of adriamycin (Fig. 8*B*).

Discussion

Microsomal PGES-1 was determined in three human prostate cancer cell lines (DU145, PC3, LNCaP), all originally derived from metastases. DU145 and PC3 do not express the androgen receptor, whereas LNCaP does (20). Relatively high expression of MPGES-1 was found for DU145, was found less in PC3, and was not detectable in LNCaP. Thus, in DU145, constitutive expression of MPGES-1 protein was more abundant than observed for the lung cancer cell line A549 stimulated with IL-1β. By immunofluorescence, perinuclear colocalization of MPGES-1 and COX-2 was evident for A549 cells after treatment with IL-1β. This cytokine also augmented the perinuclear staining for MPGES-1 in DU145 cells. Because Western blot analysis showed similarly high expression of MPGES-1 in DU145, with and without treatment with IL-1β, this suggests that the proinflammatory cytokine leads to accumulation of MPGES-1 around the nucleus.

MPGES-1 was expressed also in prostate cancer tissues. In the limited number of samples (five cancer and five benign), MPGES-1 appeared more abundant in cancer compared with benign prostate hyperplasia. There was no obvious correlation with the expression of COX-2 or androgen receptor. The MPGES-1 expression varied between the cancer samples, but this could reflect the presence of other cells in the tumors. It also seems possible that the varying MPGES-1 expression in the tumor samples may reflect the very diverse MPGES-1 expression in the three prostate cancer cell lines.

RNAi using siRNA is often partial. A strength with our study (using shRNA) is the stable and practically complete knockdown of MPGES-1, both in a tumor cell line with high constitutive expression (DU145) and in tumor cells where MPGES-1 is highly inducible (A549). When the knockdown clones were tested in clonogenic assay, these gave slower-growing colonies, reflecting a less-malignant phenotype. Injection of MPGES-1 knockdown clones to nude mice resulted in delayed tumor development and/or growth compared with WT cells. Also, the histological characterization of tumors from DU145 MPGES-1 knockdown cells showed disintegraton of the tumor parenchyma, with severe necrosis and nonviable tissue. Proliferating tumor cells (Ki-67^+) were present only in the tumor periphery. The delayed growth of xenograft tumors from injected MPGES-1 knockdown clones suggests a reduced capacity of the cancer cells to establish and proliferate at the injection site. This is in line with COX inhibitors causing reduced invasion of DU145 and PC3 through Matrigel and reduced release of matrix metalloproteases (21). The low viability of tumors growing from knockdown cells may also depend on defective angiogenesis; PGE_2 leads to VEGF release in prostate cancer cell lines (22).

Previously, COX-2 expression was reduced with shRNA in the breast cancer cell line LM2–4175, and tumor growth in immunocompromised mice was monitored (23). For these cells, knockdown only of COX-2 gave a limited effect; however, combined knockdown of four genes (COX-2, epiregulin, MMP1/2) almost completely abrogated tumor growth. In comparison, it thus appears that MPGES-1 knockdown gives a more pronounced effect than separate COX-2 knockdown. In addition to cell type-specific PGE_2 requirements, a possible reason may be that COX-2 knockdown cells can be supplied with PGH_2 from stroma cells by transcellular metabolism (24). A549 cells were recently found to metabolize PGH_2 derived from HUVECs (25). Furthermore, although COX-2 is generally assumed to be the major PGH_2 producer in tumors (8, 10), there is also evidence of a role for COX-1. Thus, knockdown of COX-1 in the cervix carcinoma cell line Hep2 reduced PGE_2 formation (26), and COX-1 is weakly expressed in, for example, DU145 cells (18). PGE_2 may thus be formed in cancer cells lacking COX-2.

An interesting question is whether PGE_2 formed by other cells in the tumor tissue may promote tumor growth, as does PGE_2 produced by the cancer cells (6). Xenograft tumors deriving from the MPGES-1 knockdown clones (both DU145 and A549) expressed MPGES-1, probably reflecting the presence of other cell types (stroma, vessels, leukocytes) in the tumor tissue. In addition, COX-2 was present in all tumors. Furthermore, COX-1 and the other two PGE synthases may be expressed in the cancer cells as well as in stromal cells of the xenografts. Thus, PGE_2 could potentially be formed also in the MPGES-1 knockdown xenografts. Nevertheless, growth of xenograft tumors from both A549 and DU145 knockdown clones in nude mice was compromised. These observations suggest that expression of MPGES-1 in the cancer cells of tumor tissue is important and cannot be entirely substituted by PGE synthases in the stromal compartment of the tumor. This conclusion is supported by Kamei et al. (27), who found that HEK293 cells transfected with COX-2 and MPGES-1 became tumorigenic, whereas this was not the case for HEK293 cells treated with PGE_2.

COX-2 can be up-regulated by p53, and this was shown to reduce apoptosis induced by genotoxic stress (28). Also, celecoxib potentiated the effect of adriamycin on neuroblastoma tumors (29). We found that knockdown of MPGES-1 led to increased adriamycin-induced apoptosis of DU145 cells in culture, and that exogenous PGE_2 could rescue against this adriamycin-induced cell death. DU145 cells express two of the four PGE_2 receptors (EP2 and EP4) (30). These receptors are usually associated with the plasma membrane, but EP4 and EP3a have also been localized in the nuclear

envelope (of porcine brain endothelial cells) (31). A possible explanation for the observation that MPGES-1 expression is needed for DU145 (or A549) cells to proliferate in a xenograft tumor may be that endogenous formation of PGE_2, stimulating receptors within the tumor cell, is required. On the other hand, apparent stimulation of plasma membrane receptors with exogenous PGE_2 was sufficient to rescue DU145 cells against the effects of adriamycin in cell culture.

Recently, the role of MPGES-1 in intestinal tumorigenesis in Apc-mutant mice was studied by genetic deletion (knockout). Contradictory results were reported: one group observed marked and persistent suppression of cancer growth, whereas another group found that knockout gave more and larger intestinal tumors (32, 33). These mixed observations may result from deletion of MPGES-1 in all cells of the organism, possibly in combination with different experimental conditions. Our data strongly support that high expression of MPGES-1 in the cancer cell promotes growth and survival, and that inhibition of MPGES-1 is a therapeutic option for cancers that express this enzyme.

Materials and Methods

Generation of Stable MPGES-1 Knockdown Cells. Prostate cancer cell lines DU145 and non-small cell lung carcinoma cell line A549 were transfected with shRNA plasmids by using Lipofectamine 2000 (Invitrogen). Stably transfected clones were isolated with puromycine (8 μg/mL). The sequence of the shRNA insert is: 5′-CCGGGAACGACATGGAGACCATCTACTCGAGTAGATGGTCTCCATGTCGTTCTTTTTG-3′, and underlined residues correspond to nucleotides 236–258 in MPGES-1 mRNA.

Immunoblot Analysis. Cell and tissue samples were dissolved in mammalian protein extraction reagent (M-PER) with Complete protease inhibitor mixture (Roche).

Quantitative Real-Time PCR. Total RNA was extracted from cells with TRIzol (Invitrogen), and cDNA synthesis was performed by using oligo(dT) primers.

PGE_2 Synthase Activity Assay. Cells were detached from culture dishes and sonicated on ice. After centrifugation, microsomal pellet fractions were incubated with PGH_2 (10 μM) for 1 min on ice. After solid-phase extraction, samples were analyzed by reverse-phase HPLC.

Fluorescence Microscopy. DU145 and A549 cells growing on chamber slides were fixed with methanol at −20 °C for 5 min. Samples were incubated with anti-MPGES-1 and anti-COX-2 antisera, and fluorescent secondary antibodies and were analyzed with an LSM 510 Laser Scanning Microscope (Carl Zeiss).

Clonogenic Assay. To determine colony formation, DU145 and A549 cells were seeded (150 cells per well) in six-well plates. After 12 days, colonies (>75 cells) with 50% plate efficiency were counted.

Animals and Xenografting. Female NMRI nu/nu mice (4–8 weeks old) were s.c. injected in both hind flanks with the following tumor cell variants: 2×10^6 DU145 WT, DU145 nontarget shRNA control, or DU145 MPGES-1 knockdown clone A. For the same variants of A549, 5×10^6 cells were injected. A tumor was considered to be established once it had reached a volume of 0.2 mL. For immunohistochemical analysis, sections from paraformaldehyde-fixed, paraffin-embedded tissue were incubated with primary antibody Ki-67.

Human Prostate Samples. Prostate specimens were obtained (fresh frozen) from prostate cancer patients undergoing radical prostatectomy. Histopathological staining confirmed the presence of tumor or benign tissue. Cancer samples were graded by using the Gleason score (Table 1).

Apoptosis and Cell Viability Assays. Cytokeratin 18 fragments in cell lysates were determined by ELISA. The appearance of activated caspase-3 was confirmed by Western blotting. Cell viability was determined by mitochondrial dehydrogenase assay (cleavage of the tetrazolium salt WST-1).

Additional Information. For more detailed information on all *Materials and Methods*, see *SI Materials and Methods*.

ACKNOWLEDGMENTS. We thank Johan Dixelius and Christer Betsholtz for kind help and access to LSM 510. This work was supported by the Swedish Research Council, European Union Grants LSHM-CT-2004-00533 and FP7-Health-201668, the Swedish Children's Cancer Foundation, the Stockholm Cancer Society, and the Swedish Cancer Foundation. H.H. was supported by the Nakatomi Foundation, the Naito Foundation, the Scandinavia-Japan Sasakawa Foundation, and the Nakayama Foundation for Human Science.

1. Jakobsson PJ, Morgenstern R, Mancini J, Ford-Hutchinson A, Persson B (2000) Membrane-associated proteins in eicosanoid and glutathione metabolism (MAPEG)–a widespread protein superfamily. *Am J Respir Crit Care Med* 161:S20–S24.
2. Jakobsson PJ, Thoren S, Morgenstern R, Samuelsson B (1999) Identification of human prostaglandin E synthase: A microsomal, glutathione-dependent, inducible enzyme, constituting a potential novel drug target. *Proc Natl Acad Sci USA* 96:7220–7225.
3. Murakami M, et al. (2000) Regulation of prostaglandin E-2 biosynthesis by inducible membrane-associated prostaglandin E-2 synthase that acts in concert with cyclooxygenase-2. *J Biol Chem* 275:32783–32792.
4. Thoren S, Jakobsson PJ (2000) Coordinate up- and down-regulation of glutathione-dependent prostaglandin E synthase and cyclooxygenase-2 in A549 cells–inhibition by NS-398 and leukotriene C-4. *Eur J Biochem* 267:6428–6434.
5. Samuelsson B, Morgenstern R, Jakobsson PJ (2007) Membrane prostaglandin E synthase-1: A novel therapeutic target. *Pharmacol Rev* 59:207–224.
6. Greenhough A, et al. (2009) The COX-2/PGE2 pathway: Key roles in the hallmarks of cancer and adaptation to the tumour microenvironment. *Carcinogenesis* 30:377–386.
7. Werz O, Steinhilber D (2006) Therapeutic options for 5-lipoxygenase inhibitors. *Pharmacol Ther* 112:701–718.
8. Cha YI, DuBois RN (2007) NSAIDs and cancer prevention: Targets downstream of COX-2. *Annu Rev Med* 58:239–252.
9. McCarty MF (2004) Targeting multiple signaling pathways as a strategy for managing prostate cancer: Multifocal signal modulation therapy. *Integr Cancer Ther* 3:349–380.
10. Patel MI, Kurek C, Dong Q (2008) The arachidonic acid pathway and its role in prostate cancer development and progression. *J Urol* 179:1668–1675.
11. Zha S, et al. (2001) Cyclooxygenase-2 is up-regulated in proliferative inflammatory atrophy of the prostate, but not in prostate carcinoma. *Cancer Res* 61:8617–8623.
12. St Sauver JL, Jacobson DJ, McGree ME, Lieber MM, Jacobsen SJ (2006) Protective association between nonsteroidal antiinflammatory drug use and measures of benign prostatic hyperplasia. *Am J Epidemiol* 164:760–768.
13. Patel MI, et al. (2008) Cytosolic phospholipase A2-alpha: A potential therapeutic target for prostate cancer. *Clin Cancer Res* 14:8070–8079.
14. Castellone MD, Teramoto H, Gutkind JS (2006) Cyclooxygenase-2 and colorectal cancer chemoprevention: The beta-catenin connection. *Cancer Res* 66:11085–11088.
15. Serafini P, Borrello I, Bronte V (2006) Myeloid suppressor cells in cancer: Recruitment, phenotype, properties, and mechanisms of immune suppression. *Semin Cancer Biol* 16:53–65.
16. Wang MT, Honn KV, Nie D (2007) Cyclooxygenases, prostanoids, and tumor progression. *Cancer Metastasis Rev* 26:525–534.
17. Johnsen JI, et al. (2005) NSAIDs in neuroblastoma therapy. *Cancer Lett* 228:195–201.
18. Subbarayan V, Sabichi AL, Llansa N, Lippman SM, Menter DG (2001) Differential expression of cyclooxygenase-2 and its regulation by tumor necrosis factor-alpha in normal and malignant prostate cells. *Cancer Res* 61:2720–2726.
19. Fadeel B, Ottosson A, Pervaiz S (2008) Big wheel keeps on turning: Apoptosome regulation and its role in chemoresistance. *Cell Death Differ* 15:443–452.
20. Lau KM, LaSpina M, Long J, Ho SM (2000) Expression of estrogen receptor (ER)-alpha and ER-beta in normal and malignant prostatic epithelial cells: Regulation by methylation and involvement in growth regulation. *Cancer Res* 60:3175–3182.
21. Attiga FA, Fernandez PM, Weeraratna AT, Manyak MJ, Patierno SR (2000) Inhibitors of prostaglandin synthesis inhibit human prostate tumor cell invasiveness and reduce the release of matrix metalloproteinases. *Cancer Res* 60:4629–4637.
22. Jain S, Chakraborty G, Raja R, Kale S, Kundu GC (2008) Prostaglandin E2 regulates tumor angiogenesis in prostate cancer. *Cancer Res* 68:7750–7759.
23. Gupta GP, et al. (2007) Mediators of vascular remodelling co-opted for sequential steps in lung metastasis. *Nature* 446:765–770.
24. Folco G, Murphy RC (2006) Eicosanoid transcellular biosynthesis: From cell-cell interactions to in vivo tissue responses. *Pharmacol Rev* 58:375–388.
25. Salvado MD, Alfranca A, Escolano A, Haeggstrom JZ, Redondo JM (2009) COX-2 limits prostanoid production in activated HUVECs and is a source of PGH2 for transcellular metabolism to PGE2 by tumor cells. *Arterioscler Thromb Vasc Biol* 29:1131–1137.
26. Radilova H, et al. (2009) COX-1 is coupled with mPGES-1 and ABCC4 in human cervix cancer cells. *Mol Cell Biochem*, in press.
27. Kamei D, et al. (2003) Potential role of microsomal prostaglandin E synthase-1 in tumorigenesis. *J Biol Chem* 278:19396–193405.
28. Han JA, et al. (2002) P53-mediated induction of Cox-2 counteracts p53- or genotoxic stress-induced apoptosis. *EMBO J* 21:5635–5644.
29. Ponthan F, et al. (2007) Celecoxib prevents neuroblastoma tumor development and potentiates the effect of chemotherapeutic drugs in vitro and in vivo. *Clin Cancer Res* 13:1036–1044.
30. Wang X, Klein RD (2007) Prostaglandin E2 induces vascular endothelial growth factor secretion in prostate cancer cells through EP2 receptor-mediated cAMP pathway. *Mol Carcinog* 46:912–923.
31. Bhattacharya M, et al. (1999) Localization of functional prostaglandin E2 receptors EP3 and EP4 in the nuclear envelope. *J Biol Chem* 274:15719–15724.
32. Elander N, et al. (2008) Genetic deletion of mPGES-1 accelerates intestinal tumorigenesis in APC(Min/+) mice. *Biochem Biophys Res Commun* 372:249–253.
33. Nakanishi M, et al. (2008) Genetic deletion of mPGES-1 suppresses intestinal tumorigenesis. *Cancer Res* 68:3251–3259.